Numerical study on wake recovery of vertical-axis wind turbines through fixed blade pitch offsets

H vs X rotors

Ajay, Adhyanth Giri; Ferreira, Carlos Simao

DOI
10.1088/1742-6596/2767/7/072010

Publication date
2024

Document Version
Final published version

Published in
Journal of Physics: Conference Series

Citation (APA)
Ajay, A. G., & Ferreira, C. S. (2024). Numerical study on wake recovery of vertical-axis wind turbines through fixed blade pitch offsets: H vs X rotors. *Journal of Physics: Conference Series*, *2767*(7), Article 072010. https://doi.org/10.1088/1742-6596/2767/7/072010

Journal of Physics: Conference Series

PAPER • **OPEN ACCESS**

Numerical study on wake recovery of vertical-axis wind turbines through fixed blade pitch offsets: H vs X rotors

To cite this article: Adhyanth Giri Ajay and Carlos Simao Ferreira 2024 *J. Phys.: Conf. Ser.* **2767** 072010

Journal of Physics: Conference Series **2767** (2024) 072010 doi:10.1088/1742-6596/2767/7/072010

Numerical study on wake recovery of vertical-axis wind turbines through fixed blade pitch offsets: H vs X rotors

Adhyanth Giri Ajay, Carlos Simao Ferreira

Wind Energy Section, Flow Physics and Technology, Faculty of Aerospace Engineering, Delft University of Technology, Delft 2629HS, The Netherlands.

E-mail: A.GiriAjay@tudelft.nl

Abstract. This study assesses the wake recovery mechanism between an H-type Darrieus and an X-type vertical-axis wind turbine, named H-Rotor and X-Rotor respectively for different blade pitch offset configurations. The analysis is conducted in OpenFOAM using the actuator line method to model the turbines to present qualitative (velocity and vorticity contours) and quantitative (available power) studies for three different fixed blade pitch offsets. The results demonstrate that the H-Rotor recovers the wake much faster than the X-Rotor at positive pitch offsets. Overall, applying fixed pitch offsets to VAWT blades helps recover the wake faster than having no blade pitch offset.

1. Introduction

Vertical-axis wind turbines (VAWTs) have been shown to have the potential to significantly increase the power density of wind farms [1]. Indicating this potential, new VAWT configurations are being constantly developed. One such new VAWT design is the X-Rotor [2], which is designed to reduce the LCoE of turbines (Figure 1). This design deviates from a traditional VAWT geometry by including two sets of coned blades in an "X" shape configuration (primary rotors), that extract energy from the wind, with tip-mounted horizontal-axis wind turbines that generate electrical power (secondary rotors). The design involves pitch-controlled upper blades that are designed to shed aerodynamic power in above-rated conditions. The lower blades are not pitch-controlled as it would disrupt the operation of the secondary rotors. The scope of the present study is two-fold: (1) to study the near- and far-wake of this X-Rotor rotor to understand the vortex system behind its wake recovery and, (2) to compare this wake recovery with that of a more traditional Darrieus H-type VAWT (henceforth referred to as H-Rotor).

Numerical, experimental, and field investigations concerning Vertical Axis Wind Turbines (VAWTs) have consistently demonstrated a notably accelerated wake recovery, achieving 95% freestream velocity, in comparison to Horizontal Axis Wind Turbines (HAWTs) [3, 4]. This phenomenon is predominantly ascribed to the heightened turbulent mixing within VAWTs, augmented secondarily by the vertical advection of wake attributed to the streamwise tip vortices [5, 6, 7]. Notably, Jadeja[8] substantiated the augmentation of wake deflection through numerical simulations by introducing blade pitching in VAWTs, resulting in amplified magnitudes of streamwise vortices, without significant loss in rotor power. The outcomes revealed that fixed

pitch offsets influenced the loading distribution, showing dominance to either the upwind or downwind half depending on the pitch direction. This phenomenon was further corroborated experimentally by Huang et. al.[9]. Huang[10] subsequently delved into an in-depth numerical analysis of the wake dynamics in three-bladed full-size H-type VAWTs, encompassing both an isolated turbine case and a scenario with three turbines arranged in-line. The findings disclosed substantial enhancements in the wake recovery process, ranging from 35% to 45%, in contrast to blades without pitch offsets, with only 6 to 9% single turbine power loss with blade pitch.

With the X-Rotor being a new VAWT concept, the wake and wake recovery studies are quite primitive, yet. However, recent experimental work on a scaled version of the primary rotor described the rotor loading and the 3D aerodynamics inside its volume [11]. This work revealed that the coned blades induce significant three-dimensionality in the aerodynamics, as the shed vorticity (at downstream planar locations) is extremely elliptical, in contrast to the straight line of H-Rotors. A numerical study on the full-scale primary rotor showed that operating the X-Rotor with fixed pitch offsets significantly changes the vertical induction inside the volume of the rotor [12], with a 10 - 12% power loss with pitch angles of 10° and -10°. However, there is still a gap in knowledge about the vortex system of this rotor at far-wake locations and how it changes while operating at different fixed pitch offsets.

This work is a first step towards quantifying the farm-level aerodynamics of the X-Rotor and understanding its performance in comparison to an H-Rotor. In this study, both rotors are simulated at different fixed blade pitch offsets and the analyses focus on the influence of the vortices on the wake deformation as well as the available power at different downstream and lateral locations.

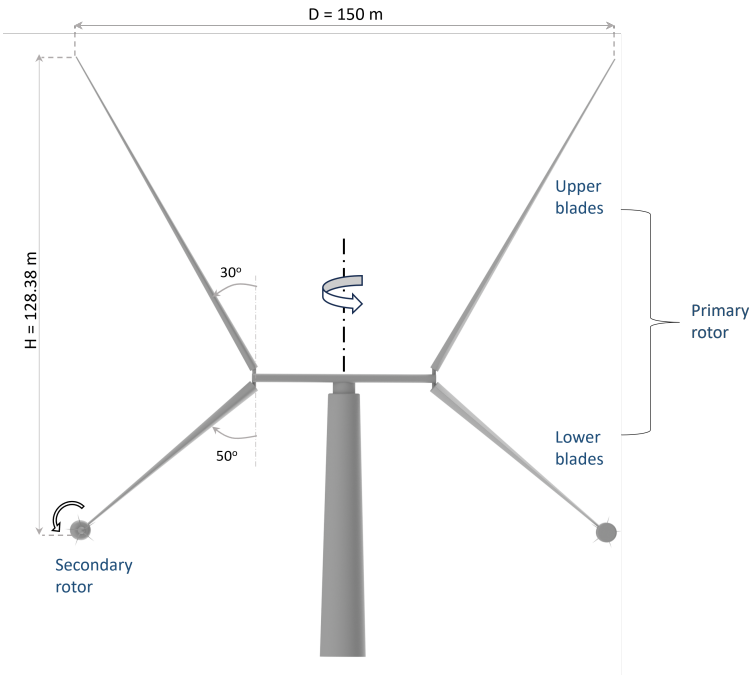

Figure 1: A render of the X-Rotor turbine with geometrical dimensions from [2].

2. Methodology

2.1. Test geometry

To compare two rotors of different geometry, the rotors should be scaled to produce similar thrust. Therefore, the two-bladed H-Rotor is constructed to match the frontal area (A),

solidity(σ), and rotor aspect ratio (AR) of the X-Rotor under the same operating conditions (inflow velocity (U) and tip-speed ratio (λ)). The secondary rotors are not included in the simulation of the primary rotor to enable a more direct comparison in the rotor scale. The two turbines' geometry and operating specifications are shown in Table 1. The tower is ignored in both rotor configurations to include only the lift-producing surfaces.

Table 1: Geometry of the two rotor configurations.

Rotor type	D (m)	AR	σ	A (m^2)	U ($m\,s^{-1}$)	λ
X-Rotor	150.000	0.857	0.223	12870	12	4
H-Rotor	122.550	0.857	0.223	12870	12	4

NACA0021 polars at chord Reynolds number $Re = 1.5 \times 10^7$ are generated using XFOIL and are used for the H-Rotor turbine. The X-Rotor has tapered blades with NACA0025 at the roots and NACA0008 at the tips of both upper and lower blades at the same Re value of 1.5×10^7(constant product of relative speed and chord at each blade section). The solidity σ mentioned for this rotor is based on the mean chord value of the upper blade and the lower blade. The detailed geometry of the X-Rotor is described by Giri Ajay[12].

2.2. Model and setup

To accurately model the wake and the flow features in the domain of the VAWTs, computational fluid dynamics (CFD) is essential. In this study, the actuator line method (ALM) implementation used is *turbinesFoam* [13] coupled with the *pimpleFoam* solver in *OpenFOAM v2106*. The fluid domain simulated for the rotor spans $20D$ x $8D$ x $7D$ in spanwise (X), lateral (Y), and axial (Z) directions based on the best practices for CFD of VAWTs [14]. 3-levels of unstructured castellated mesh refinement (region refinement of 1e15 distance) are conducted between -1.5D to 11D in X, -1.5D to 1.5D in Y and Z, resulting in 7.35 million cells total. Boundary level refinement is unnecessary here, as the turbine is not treated as a wall-surface in the ALM approach. A constant, uniform inlet velocity of $U_\infty = 12\,m\,s^{-1}$ is used with a *fixedInlet* boundary condition. An unsteady-RANS turbulence model with the $\kappa - \epsilon$ closure model is used with a very low turbulence intensity ($< 0.1\%$). The rotors are placed at $5D$ downstream of the inlet to avoid pressure gradient issues at the inlet. The simulations are run for 3Ω seconds (roughly 76 revolutions) for each case, where Ω is the time taken for freestream to travel between inlet and outlet. Time-averaged results are obtained from a time of 1.5Ω with an interval of 0.2Ω, as the flow near the outlet would have relatively stabilised.

Three different pitch offsets ($-10°$, $0°$, and $+10°$) of the blade (upper only for X-Rotor) are considered for each turbine as shown in Figure 2.

No dynamic stall models are used in this study as tuning the coefficients of the Leishman-Beddoes dynamic stall model would be different for both rotors. Neglecting dynamic stall can impact the regions close to the root with positive and negative pitch angles, which might reduce any differences observed between the rotors slightly. Additionally, flow curvature models are also ignored as it would be difficult to predict its impact on the coned blades of the X-Rotor.

3. Results

3.1. Velocity fields and vortex system

The time-averaged streamwise velocity and vorticity contours of H- and the X-Rotor VAWTs at the downwind planes $X/D = 1$, 3, 5, and 7 are shown in Figure 3, Figure 4, and Figure 5 for the pitch cases $\beta = 0°$, $10°$, and $-10°$ respectively. Black dashed lines depict the frontal area of both the rotors at an azimuth of $0°$ and a black contour represents 95% of freestream (U_∞), i.e., where wake recovery is attained. The windward side of the rotor is represented as $Y/D > 0$,

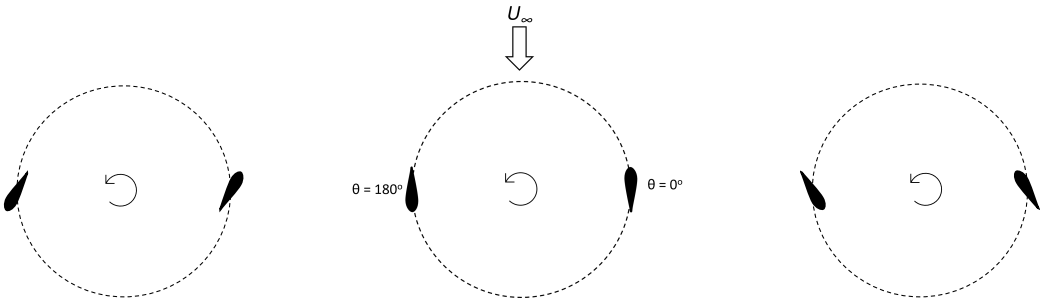

(a) Negative pitch offset (b) No pitch offset (c) Positive pitch offset

Figure 2: Top view of upper blade pitch offsets. θ indicates the azimuth and U_∞ is the freestream velocity. $\theta = 90°$ to $270°$ is the leeward side, and the other half is the windward side.

and the leeward side is $Y/D < 0$. Both the rotors are centred at $Y/D = 0$ and the root section of the X-Rotor where the upper and lower blades meet is at $Z/D = 0$. The nomenclature of the vortices in the figures follows the rotor type with location descriptors in the subscript. For instance, $H_{w,t}$ would indicate the windward top vortex of the H-Rotor, and $X_{l,b}$ would refer to the leeward bottom vortex of the X-Rotor.

At $\beta = 0°$ (Figure 3), both rotors show an axial expansion of the wake with the X-Rotor exhibiting asymmetric expansion. While the H-Rotor shows lateral contraction in the windward direction, the X-Rotor does not clearly show it at the near-wake planes. This is due to the dominant tip-vortices of the H-Rotor at the top and bottom ($H_{w,t}$ and $H_{w,b}$), while the X-Rotor does not show a dominant vortex pair. At further downstream locations, it becomes clear that the X-Rotor shows lateral contraction close to the blade tips and a lateral expansion close to the roots. This behaviour of the X-Rotor is attributed to the presence of both shed and trailing vortices close to the root region ($X_{w,r}$), driving the wake laterally outwards. This root vortex arises due to circulation conservation along the upper blade and the lower blade. At the same time, the contraction near the tips is due to the tip vortices generated from the upper and lower blades ($X_{w,t}$ and $X_{w,b}$). The vortices of both rotors diffuse at far downstream locations ($X/D \geq 5$) and turbulent mixing becomes the dominant driver of the wake recovery process. The H-Rotor has faster axial expansion than the X-Rotor due to $H_{w,t}$ and $H_{w,b}$. It also recovers the wake faster than the X-Rotor, as the velocity deficit inside the frontal area is lesser from $X/D = 3$ and beyond. Although, at $X/D = 7$ as the two dominant vortices of the H-Rotor propel each other leeward, the wake that has expanded axially is now being sucked back into the region of the frontal area.

With the $\beta = 10°$ (Figure 4) case, the wake appears to be very different than that of $\beta = 0°$. At $X/D = 1$, there is a large lateral outward expansion on both the windward and leeward direction of the H-Rotor accompanied by a significant axial contraction, pulling the freestream from above and below the frontal area of the rotor. This is attributed to the immensely strong vortex pair of $H_{w,t}$ and $H_{w,b}$ that pushes the wake out on the windward side and the weaker pair $H_{l,t}$ and $H_{l,b}$ on the leeward side. The change in vortex strength due to blade pitch is due to the change in forcefield over the rotor, as previously discussed by Huang [9]. From the vortex system of the X-Rotor, it is clear that there is a strong upper blade tip-vortex $X_{w,t}$ and a moderately strong root vortex $X_{w,r}$. The lower blade tip-vortex $X_{w,b}$ has similar strength as at $\beta = 0°$, due to the lack of pitch control. This results in the X-Rotor showing lateral expansion and axial contraction in the upper half while exhibiting lateral contraction and axial expansion in the lower half. The wake in the upper half also moves slightly upwards as $X_{w,t} > X_{w,r}$ in magnitude. As the vortices advect further downwind, it is observed that the wake of the H-Rotor

moves out of the frontal area much faster than the X-Rotor. The vortex pairs of the H-Rotor, having equal strength, mutually propel each other away from the rotor region while inducing a vertical flow in the frontal area, bringing freestream from above and below the rotor. In the X-Rotor, as $X_{w,r}$ is induced upwards by the dominant $X_{w,t}$, they induce an induced velocity in the windward direction pushing the wake out. This helps recover the wake in the upper half, but the lower half remains fairly stagnant at each downstream location. Therefore, while $X_{w,r}$ and $X_{w,t}$ start to recover the wake around $X/D = 5$, they begin diffusing and thus do not eject most of the wake out of the system. Regardless, in this pitch configuration, the H-Rotor outperforms the X-Rotor by recovering most of the wake around $X/D = 3$.

Finally, in the $\beta = -10^\circ$ (Figure 5) configuration, the vortex system of the H-Rotor appears to be a more strengthened version of the $\beta = 0^\circ$ case at $X/D = 1$. Due to this, it experiences a large lateral contraction and an axial expansion. The X-Rotor's vortex system indicates a strong $X_{w,t}$ and a moderately strong $X_{w,r}$, similar to the $\beta = 10^\circ$ case but in opposite direction. This invokes a large lateral contraction in the upper half but shows lateral expansion in the lower half, accompanied by axial expansion in both halves. As the flow moves further downwind, the windward vortex pair of both the rotors advect to the leeward side due to mutual induction between the top and bottom vortices. This process is slower in the X-Rotor than in the H-Rotor. At $X/D = 5$ and 7, the vortex pair $H_{w,t}$ and $H_{w,b}$ have advected beyond the rotor region on the leeward side. This induces a downward velocity in the region above the frontal area and an upward velocity in the region below the frontal area, thus bringing in the wake that was initially ejected out. This was briefly highlighted earlier, however, a big difference, in this case, is the large wake expansion on the leeward side due to the vortex pair advection. Therefore, the process reduces the velocity deficit in the rotor region compared to the $\beta = 0^\circ$ case but is much slower than the $\beta = 10^\circ$ configuration. In the X-Rotor, $X_{w,t}$ and $X_{w,r}$ appear to stagnate around $Y/D = 0$ as the vortices diffuse. This reduces its wake recovery, as most of the wake remains within the rotor even at $X/D = 7$.

3.2. Available Power (AP)

To quantify the effect of this wake recovery mechanism in each pitch configuration as well as to identify the performance ceiling of a hypothetical downstream turbine (HDT) at different locations in the lateral directions, the AP (u^3/U_∞^3) is calculated based on the streamwise velocity component in Figure 6. A laterally moving integration surface representing the rotor frontal area is used to obtain the AP for an HDT located at a lateral offset y_o/D from the centre of the simulated turbine at downstream locations $X/D = 1$, 3, 5, and 7.

Both rotors with no pitch offset have the least inline AP at all downstream positions compared to the cases with pitch offsets. At $X/D = 1$, the AP of the H-Rotor is higher than the X-Rotor with no pitch offset at $y_0/D = 0$. This can be attributed to the discussion of the weaker vortex strengths of the X-Rotor from Figure 3 from Section 3.1. The minimum AP magnitude for both these rotors without pitch offset is the same at 0.1, indicating that the difference in thrust between both rotors is very small. The inline AP of the H-Rotor is higher than the X-Rotor at the other two pitch configurations; 0.4 and 0.34 for the H-Rotor in contrast to 0.29 and 0.20 for the X-Rotor for $\beta = -10^\circ$ and $\beta = 10^\circ$ respectively. The previous discussions established that the H-Rotor advects the wake laterally much faster than the X-Rotor due to its stronger tip-vortices that work cohesively (Section 3.1). This effect is quantified here as it can be seen that the AP of the H-Rotor is lower on the leeward side for $\beta = -10^\circ$ and on the windward side for $\beta = 10^\circ$ compared to the X-Rotor.

At $X/D = 3$, the $\beta = 10^\circ$ configuration recovers the wake faster than any other configuration; the AP is 0.75 and 0.50 for the H-Rotor and X-Rotor respectively. This is attributed to the vortex system of both rotors, observed in Figure 4, allowing quick lateral expansion (only the upper half for X-Rotor). This lateral expansion is seen as the AP on the windward side is

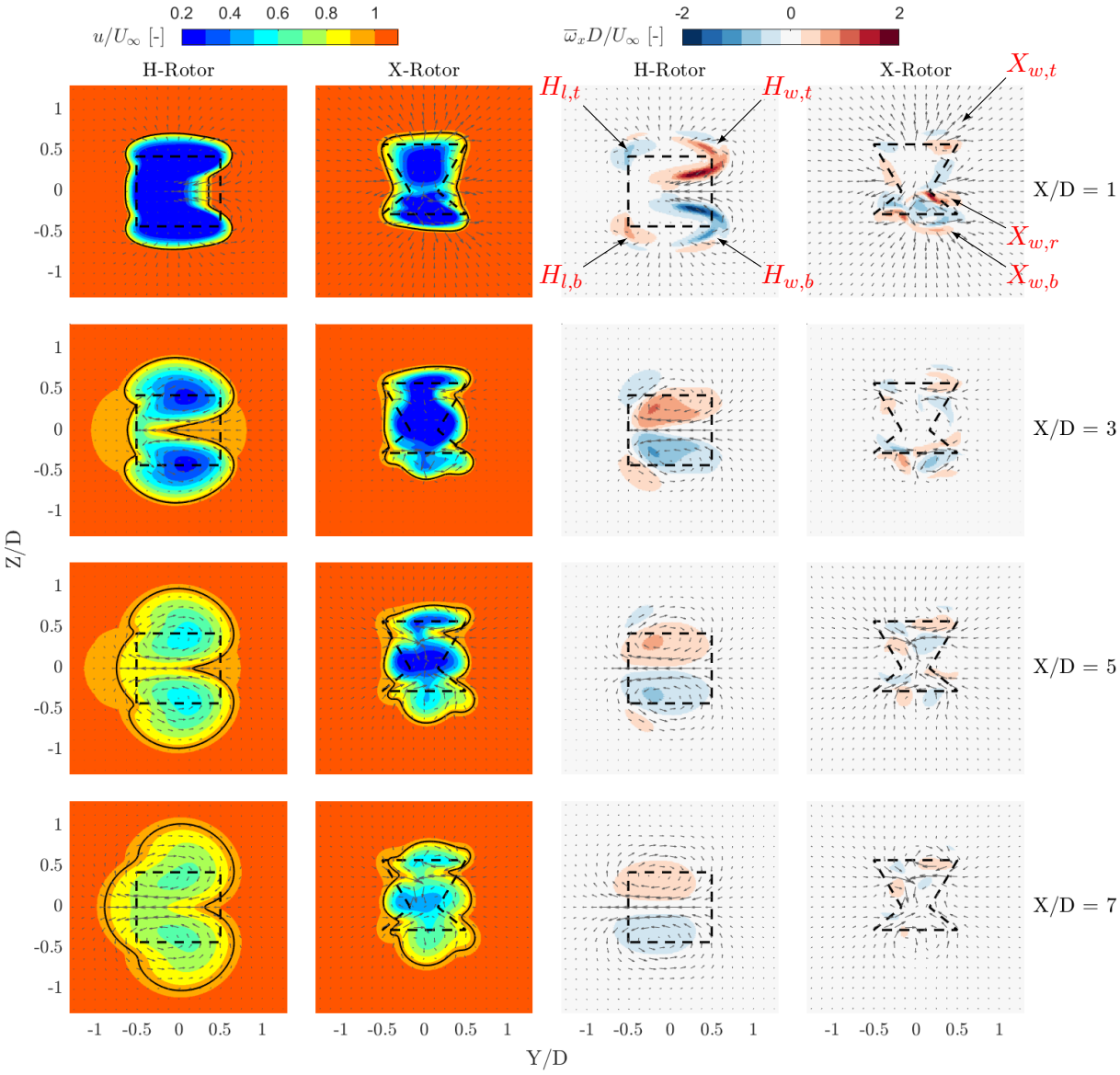

Figure 3: Normalised streamwise velocity u/U_∞ (first two columns) and the streamwise vorticity $\bar{\omega}_x D/U_\infty$ (last two columns) contours of the H-Rotor and X-Rotor with blade pitch offset $\beta = 0°$ at downstream locations $X/D = 1$, 3, 5, and 7. The black dash lines indicate the frontal area of both rotor configurations at an azimuth of 0°. The black solid contour indicates 95% U_∞. Quivers represent velocity vectors in the observed plane.

lower than at $y_0/D = 0$. The H-Rotor is significantly faster in advecting the wake as the lowest AP is 0.25 at $y_0/D = 0.93$, in contrast to the X-Rotor's 0.48 at $y_0/D = 0.4$. The $\beta = -10°$ shows a higher inline AP for the H-Rotor than the X-Rotor (0.49 versus 0.38), and the leeward advection of the H-Rotor's wake can be observed by the lower AP of 0.45 at $y_0/D = 0.33$. This expansion is lesser than the $\beta = -10°$, as the configuration also depends on the axial expansion of the wake which is not represented in the AP calculations. The X-Rotor does not show this leeward expansion as can be seen from Figure 5, the root vortex prevents the bottom half from

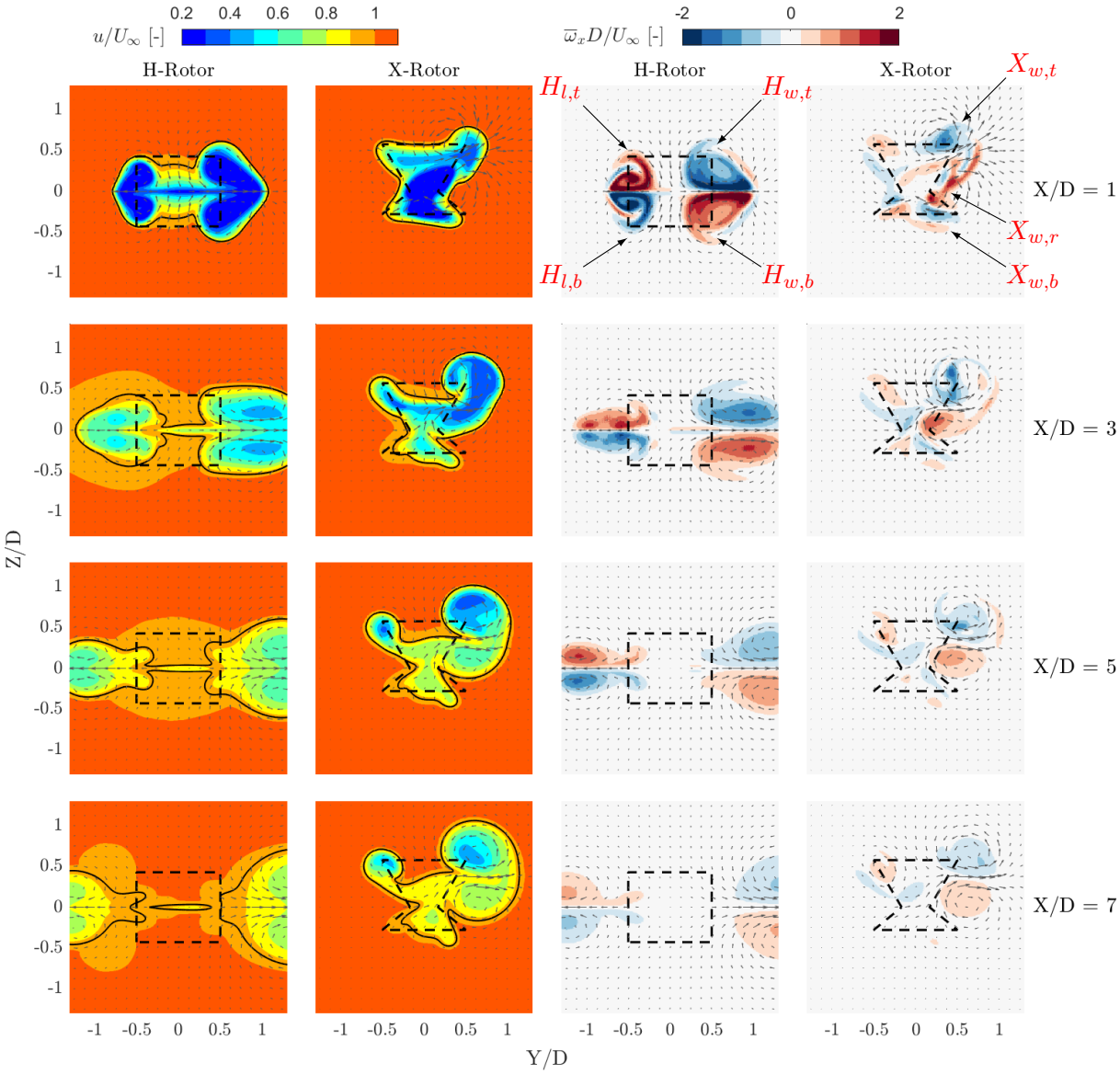

Figure 4: Normalised streamwise velocity u/U_∞ (first two columns) and the streamwise vorticity $\bar{\omega}_x D/U_\infty$ (last two columns) contours of the H-Rotor and X-Rotor with blade pitch offset $\beta = 10°$ at downstream locations $X/D = 1$, 3, 5, and 7. The black dash lines indicate the frontal area of both rotor configurations at an azimuth of 0°. The black solid contour indicates 95% U_∞. Quivers represent velocity vectors in the observed plane.

expanding in the leeward direction instead allowing axial expansion.

$X/D = 5$ is interesting as $5D$ is a common spacing between two rows of wind turbines in wind farms [15]. The inline AP of the H-Rotor with $\beta = 10°$ pitch offset is at 0.9 (implies that $u/U_\infty = 0.965$), while the X-Rotor only has an AP of 0.66. In comparison, the AP values without pitch offset are 0.43 and 0.26 for two rotors. This indicates that the H-Rotor has almost completely recovered its wake $5D$ downstream. This implies that an HDT could be placed at less than $5D$ from the first turbine, and observe improved performance compared to standard wind

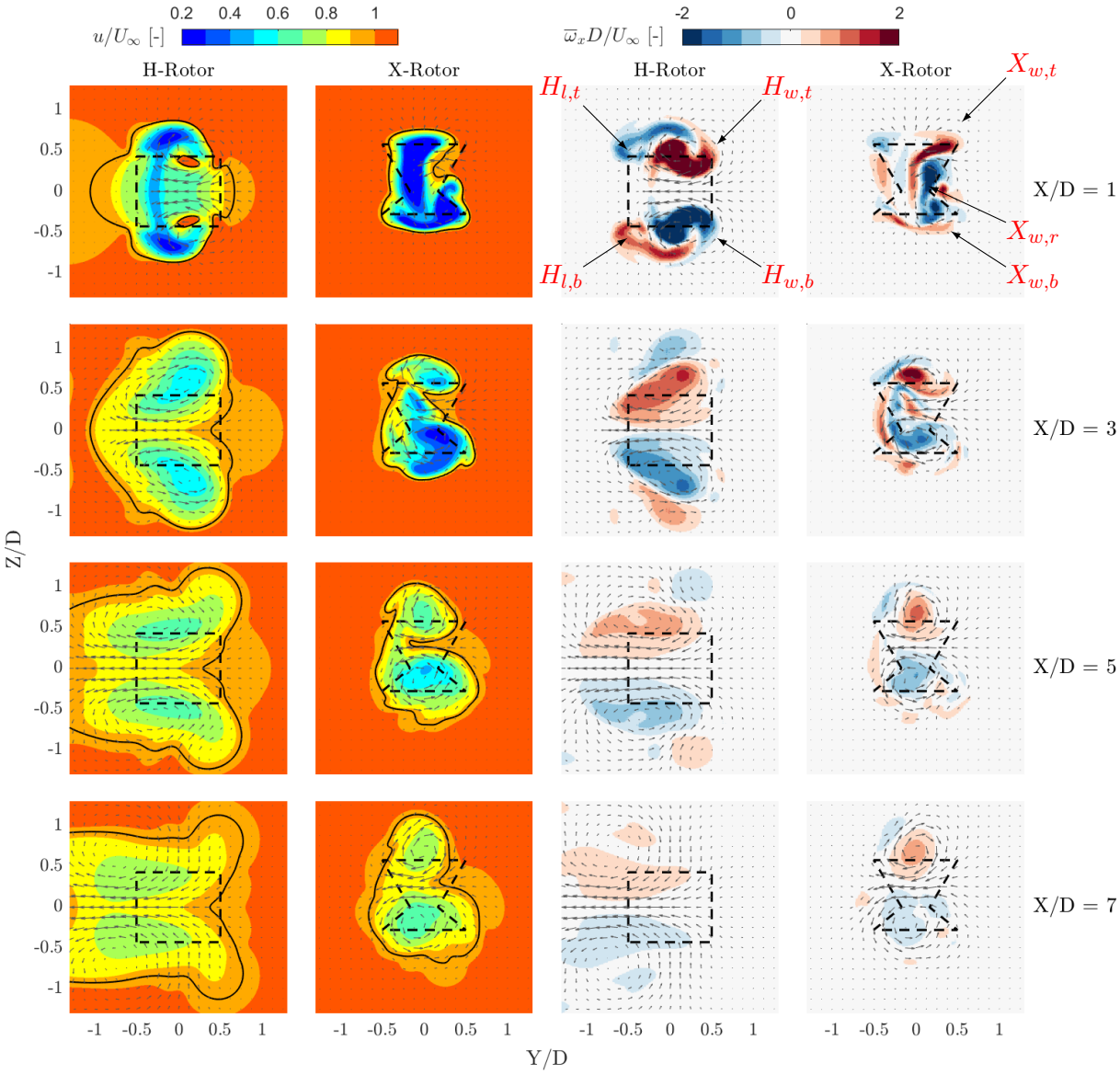

Figure 5: Normalised streamwise velocity u/U_∞ (first two columns) and the streamwise vorticity $\bar{\omega}_x D/U_\infty$ (last two columns) contours of the H-Rotor and X-Rotor with blade pitch offset $\beta = -10°$ at downstream locations X/D = 1, 3, 5, and 7. The black dash lines indicate the frontal area of both rotor configurations at an azimuth of 0°. The black solid contour indicates 95% U_∞. Quivers represent velocity vectors in the observed plane.

farm configuration. Therefore, this shows the potential to increase wind farm power density. This inline AP of the $\beta = -10°$ configuration is also higher than the values without pitch offset. At this position downstream, the wake of the H-Rotor is advected laterally beyond $y_0/D = 1$ for $\beta = 10°$ and to y_0 = -0.44 for $\beta = -10°$. This is a much faster advection than the X-Rotor, which advects the wake to y_0 = 0.58 and -0.05 for $\beta = 10°$ and 10° respectively.

At $X/D = 7$, the results look very similar to that at $X/D = 5$, except for slightly higher AP and lateral advection of the wake. This is attributed to diffusion being the dominating driver

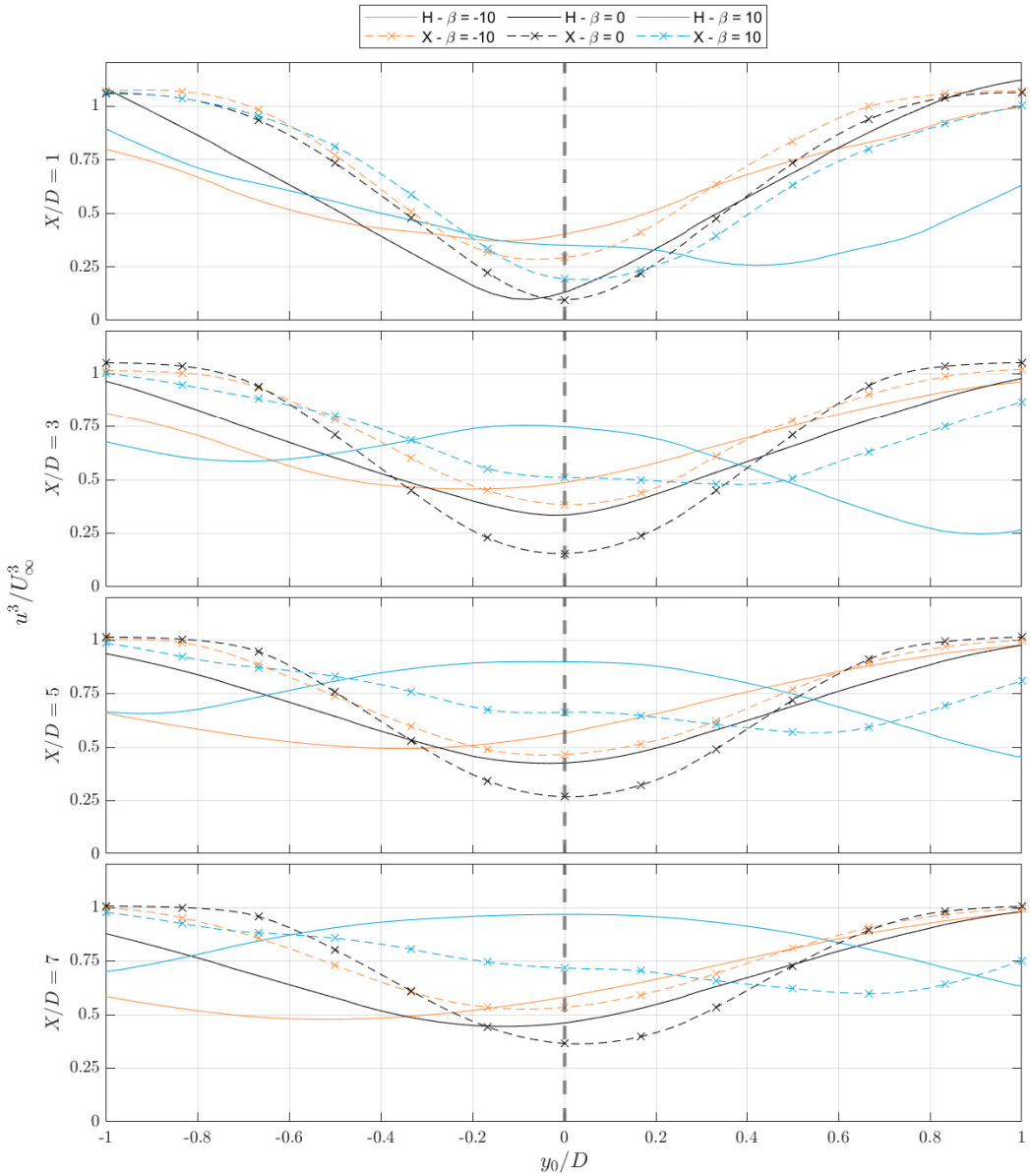

Figure 6: The available power (u^3/U_∞^3) to an HDT with a lateral displacement y_o/D at downstream locations $X/D = 1$, 3, 5, and 7 for all the pitch cases $\beta = -10°$, 0°, and 10°. Solid lines represent the HDT in a H-Rotor configuration, and the dashed lines with "X" markers show results for an HDT in the X-Rotor configuration. Black lines refers to $\beta = 0°$, while orange and cyan represent the $\beta = -10°$ and $\beta = 10°$ cases respectively. The grey dashed line at $y_0/D = 0$ highlights the results of an HDT that is inline with the original rotor.

for wake recovery over advection, which agrees with earlier discussions in Section 3.1. The $\beta = 10°$ still shows the highest wake recovery with AP values of 0.97 and 0.72 for the H-Rotor and X-Rotor compared to other configurations.

4. Conclusions and future work

A numerical study is conducted on wake recovery in VAWTs through fixed blade pitch offsets for two distinct VAWT geometries - an H-Rotor and an X-Rotor by using ALM with *OpenFOAM*. This study produced the following results:

- Blades with fixed pitch offsets ($-10°$ and $10°$ in this study) vastly improved the wake recovery process irrespective of rotor geometry
- The H-Rotor exhibited faster wake recovery than the X-Rotor at all pitch offsets. The H-Rotor with $\beta = 10°$ recovered 96.5% of the wake $5D$ downstream. The X-Rotor showed higher available power downstream of the rotor with pitch offsets than without.
- The wake recovery of the X-Rotor is hindered by the presence of root vortices, that are absent in the H-Rotor. This is due to the unequal strength between the tip of the root vortices that reduced the lateral induced velocity from the X-Rotor.

As the root vortex arises due to the circulation conservation between the upper and lower blades, pitching the lower blades could be a possible strategy to reduce the strength of the root vortices. Future work aims to study this strategy to help improve the wake recovery of the X-Rotor while also furthering our understanding of the vortex systems of such turbines.

5. Acknowledgements

The authors acknowledge the funding received from the European Union's Horizon 2020 research and innovation program under grant agreement number 101007135.

References

[1] Dabiri J O 2011 *Journal of Renewable and Sustainable Energy* **3** ISSN 19417012
[2] Leithead W, Camciuc A, Amiri A K and Carroll J 2019 *Journal of Physics: Conference Series* **1356** ISSN 17426596
[3] Shamsoddin S and Porté-Agel F 2014 *Energies* **7** 890–912 ISSN 19961073
[4] Mendoza V, Bachant P, Ferreira C and Goude A 2019 *Wind Energy* **22** 171–188 ISSN 10991824
[5] Kinzel M, Araya D B and Dabiri J O 2015 *Physics of Fluids* **27** 115102 ISSN 1070-6631
[6] Rolin V and Porté-Agel F 2015 *Journal of Physics: Conference Series* vol 625 p 012012 ISSN 17426596
[7] Chatelain P, Duponcheel M, Zeoli S, Buffin S, Caprace D G, Winckelmans G and Bricteux L 2017 *Journal of Physics: Conference Series* vol 854 p 012011 ISSN 17426596
[8] Jadeja A 2018 *Wake Deflection Technique for Vertical Axis Wind Turbines using Actuator Line Model in OpenFOAM* April
[9] Huang M, Sciacchitano A and Ferreira C 2023 *Wind Energy* 365–387 ISSN 10991824
[10] Huang M 2023 *Wake and wind farm aerodynamics of vertical axis wind turbines* Ph.D. thesis
[11] Bensason D, Sciacchitano A and Ferreira C 2023 *Journal of Physics: Conference Series* **2505** ISSN 17426596
[12] Giri Ajay A, Morgan L, Wu Y, Bretos D, Cascales A, Pires O and Ferreira C 2024 *Wind Energy Science* **9**(2) 453–470
[13] Bachant P, Goude A and Wosnik M 2016 *Wind Energy* (*Preprint* `1605.01449`)
[14] Rezaeiha A, Kalkman I and Blocken B 2017 *Renewable Energy* **107** 373–385 ISSN 18790682
[15] Flaszyński P, Wasilczuk F, Piotrowicz M, Telega J, Mitraszewski K and Hansen K S 2024 *Wind Energy* **27** 53 – 74 ISSN 10991824